J Mater Sci (2008) 43:6486–6494
DOI 10.1007/s10853-008-2978-2

Adsorption and photocatalytic decomposition of organic molecules on carbon-coated TiO_2

Tae-Won Kim · Min-Joo Lee · Wang-Geun Shim · Jae-Wook Lee · Tae-Young Kim · Dae-Haeng Lee · Hee Moon

Received: 12 May 2008 / Accepted: 29 August 2008 / Published online: 17 September 2008

Abstract Carbon-coated anatase TiO_2 samples were prepared from the mixture of poly vinyl alcohol (PVA) and commercial TiO_2 (P-25) with different mass ratios and heating temperatures. The samples were characterized by X-ray diffraction (XRD), field emission scanning electron microscope (FE-SEM), energy dispersive spectrometer (EDX), transmission electron microscope (TEM), and nitrogen adsorption analyses. The adsorption properties and photocatalytic activity of commercial and carbon-coated TiO_2 catalysts were compared for the oxidation of methylene blue (MB) and bisphenol-A (BPA). It was interesting to find that the transition from anatase to rutile was suppressed by carbon coating of TiO_2 at high temperature up to 800 °C. The carbon-coated TiO_2 samples have a higher surface area and a greater adsorption amount than commercial P-25 because of the thin layer of carbon that covered TiO_2. It was also observed that the photodecomposition efficiency was dependent on the crystallinity of the carbon-coated sample.

T.-W. Kim · W.-G. Shim · H. Moon (✉)
School of Applied Chemical Engineering, Chonnam National University, Gwangju 500-757, Korea
e-mail: hmoon@jnu.ac.kr

M.-J. Lee
R&D Center, NEXEN TIRE Corporation, Yangsan Kyungnam 626-230, Korea

J.-W. Lee
Department of Chemical and Biochemical Engineering, Chosun University, Gwangju 501-759, Korea

T.-Y. Kim
Department of Environmental Engineering, Chonnam National University, Gwangju 500-757, Korea

D.-H. Lee
Gwangju Public Health and Environmental Research Institute, Gwangju 502-240, Korea

Introduction

The degradation of organic compounds dissolved in water using a photocatalyst has attracted much attention because it is easy to handle, inexpensive, stable, and effective [1, 2]. Anatase-type of TiO_2 has been widely studied owing to its high photocatalytic activity compared to rutile type of TiO_2 [3, 4]. However, there are certain disadvantages associated with the conventional TiO_2 powdered catalyst. Namely, it is not easy to separate from solution after photocatalytic reaction, and is difficult to bind on substrate as the flat-plate or filter. Moreover, the concentration of pollutant around the TiO_2 can be lowered while the photocatalytic reaction is taking place [5].

Recently, many researchers have investigated on the composite of carbon and TiO_2 as alternative solutions for overcoming these problems. This composite between carbon and TiO_2 gives two functions: the photocatalytic activity of TiO_2 and the adsorption ability of carbon [6, 7]. In the photocatalytic oxidation process, adsorption plays a key role because high adsorption of pollutants that provide a high concentration of pollutant around the TiO_2 may induce high photocatalytic activity [8]. There are four different composition methods: TiO_2-mounted activated carbon, TiO_2 coating by metal organic chemical vapor deposition (MOCVD), carbon-doped TiO_2, and carbon-coated TiO_2 [9, 10]. Among these four methods, carbon-coated TiO_2 has been found to be the most successful catalyst that offers simultaneous adsorption and photocatalytic oxidation properties leading to enhancement of

activity [9–12]. Furthermore, the addition of activated carbon on the TiO_2 photocatalyst can prevent the recombination of electron-hole pairs as well as the reaction of TiO_2 particles with organic binders [6, 7, 13, 14]. In the carbon-coated TiO_2, the carbon layer on the surface of TiO_2 must be thin enough to transmit UV, and its adsorption capacity should be higher than that of the original TiO_2 photocatalyst. However, few studies have been reported on the photocatalytic activity of carbon-coated TiO_2 prepared by mixing TiO_2 with a carbon precursor [11, 12]. Therefore, it is necessary to understand the photocatalytic properties of the carbon-coated photocatalyst systematically.

In this work, the carbon-coated TiO_2 was prepared by heating the mixture of poly vinyl alcohol (PVA) and commercial TiO_2 (P-25) under Ar atmosphere. The samples thus prepared and the heat-treated P-25 were characterized by X-ray diffraction (XRD), field emission scanning electron microscope (FE-SEM), energy dispersive spectrometer (EDX), transmission electron microscope (TEM), and nitrogen adsorption analyses. The carbon coated TiO_2 photocatalysts and the heat-treated P-25 samples were then used for the photocatalytic degradation of methylene blue (MB) and bisphenol-A (BPA) under UV radiation.

Experimental

Synthesis and characterization of carbon-coated TiO_2 particles

Carbon-coated TiO_2 particle was prepared by using P-25 (Degussa, Germany) and PVA. The average polymerization degree of PVA used as a carbon precursor was 2000 (Duksan Pure Chemical Co. LTD, Korea). Different ratios of P-25/PVA (80/20, 90/10 and 95/5) were heated under argon atmosphere (150 mL/min) at 400, 500, 600, 700, and 800 °C for 1 h with a heating rate of 5 °C/min. For the improvement of dispersibility, the prepared samples were ground on a ball mill. The carbon-coated TiO_2 samples were characterized by powder XRD (D/MAX Uitima, Rigaku, Japan), TEM (JEOL, JEM 2000FX2), and FE-SEM·EDX (S-4700, Hitachi, Japan) and also by nitrogen adsorption-desorption isotherms at 77 K (Autosorb-1, Quantachrome Co. USA). XRD patterns were measured with CuKα radiation and at a scanning speed of 2°/min.

Adsorption and photodecomposition of MB and BPA

The adsorbates used in this study are MB (Duksan Pure Chemical Co. LTD, Korea) and BPA. The solutions were prepared with the concentration of 50 ppm. The adsorption equilibrium data were obtained by keeping the Erlenmeyer flasks containing known amounts of prepared samples in 200 mL of MB and BPA solution in a dark incubator at 25 °C for 3 days. Photodecomposition of MB was carried out on carbon-coated TiO_2 and P-25 under irradiation of 8 UV lamps (SANKYO DENKI G8T5 UV C of 8 W). The lamp emits the light in the maximum wavelength of 253.7 nm. The initial concentration of MB solution was 50 ppm. The prepared carbon-coated photocatalyst of 0.3 g was added into 1L MB solution. Similar to MB, the photodecomposition was also carried out for BPA. The pH value of MB and BPA solution was kept around 6.5–7. With an appropriate time interval, 5 mL sample solution was collected, and the concentrations of MB and BPA remaining in solutions were determined on a UV-Visible spectrophotometer (SHIMADZU, UV-1700, Japan) at 664 nm and 278 nm, respectively.

Results and discussion

Characterization

Figure 1 shows XRD patterns of P-25 and carbon-coated TiO_2 samples according to the mixing ratio and heat treatment. P-25 shows that the phase transformation from anatase to rutile increases rapidly with increasing annealing temperature above 700 °C. At 900 °C, almost all the crystal structure of TiO_2 was in rutile phase with a trace of anatase phase (Fig. 1a). In the case of 95/5 mass ratio, a phase change from antase to rutile was not observed at below 700 °C in contrast to 800 °C heat treatment conditions as shown in Fig. 1b. In addition, the anatase phase is available without much change even at 800 °C heating condition, whereas at the same heating temperature, the crystalline structure of P-25 was almost all transferred to rutile phase. Moreover, the increase of crystallinity in anatase phase appeared to be a Full Width at Half Maximum intensity (FWHM) in XRD patterns. After the heat treatment at below 800 °C, the mixture of PVA and TiO_2 appeared black in color owing to the formation of carbon-coated TiO_2, while P-25 was white in appearance. Figure 1c and d shows the XRD patterns of different TiO_2/PVA ratios (90/10and 80/20) at different heat treatment conditions (700, 800 and 900 °C). The XRD patterns of these samples prepared were almost similar. The phase transformation of anatase to rutile was observed at above 700 °C. However, the phase transformation of TiO_2 crystal structure was suppressed by increasing the PVA content. It was observed that 101 XRD peak of anatase is higher than rutile 110 peak for the samples heated at 900 °C. In other words, coated carbon restricts the phase transformation of anatase to rutile even at very high temperatures. The high

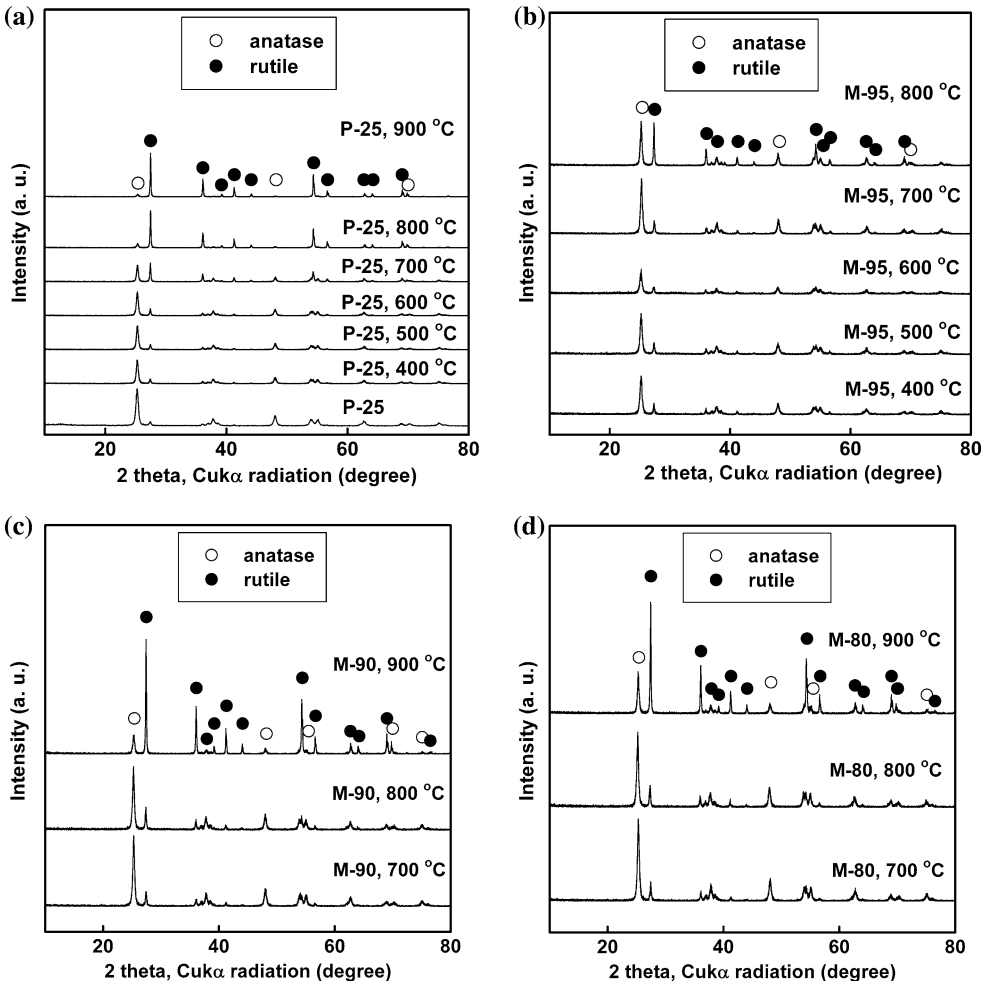

Fig. 1 XRD patterns of different heat-treated P-25 and carbon-coated TiO_2 samples: (**a**) original and heat-treated P-25; (**b**) TiO_2/PVA: 95/5 wt%; (**c**) TiO_2/PVA: 90/10 wt%; and (**d**) TiO_2/PVA: 80/20 wt%

crystallinity of anatase phase was not observed in P-25 and in lower carbon-coated TiO_2 that was treated at above 900 °C because of the phase transformation of antase to rutile. The particle size of the samples was calculated from XRD data by using Scherrer's equation,

$$L = \frac{K\lambda}{\beta \cos\theta} \tag{1}$$

where L is the particle size, λ is the wavelength of XRD (Cu Ka = 0.154 nm), K is the constant about 0.9, and β is the FWHM of 101 diffraction line of the anatase phase of each sample. The calculated particle sizes of prepared samples are listed in Table 1. For carbon-coated samples, the particle size calculated is in the range of 30 nm to 40 nm, which is bigger than the original P-25 or heated P-25, even though they were heated at the same temperature. To investigate the effects of carbon coating on the surface of TiO_2 and the adsorption abilities of the photocatalysts, the nitrogen adsorption-desorption isotherms were measured at 77 K. The nitrogen adsorption isotherms of the carbon-

Table 1 Particle size of prepared samples with Scherrer equation

Sample code	Heating temperature (°C)	TiO_2 (mass%)	PVA (mass%)	Particle size of photocatalyst (nm)	FWHM (degree)
P-25	–	100	0	25.7	0.488
M-80, 800	800	80	20	37.4	0.334
M-80, 900	900	80	20	40.1	0.312
M-90, 800	800	90	10	35.6	0.352
M-90, 900	900	90	10	28.8	0.435
M-95, 700	700	95	5	36.2	0.345
M-95, 800	800	95	5	31.0	0.403

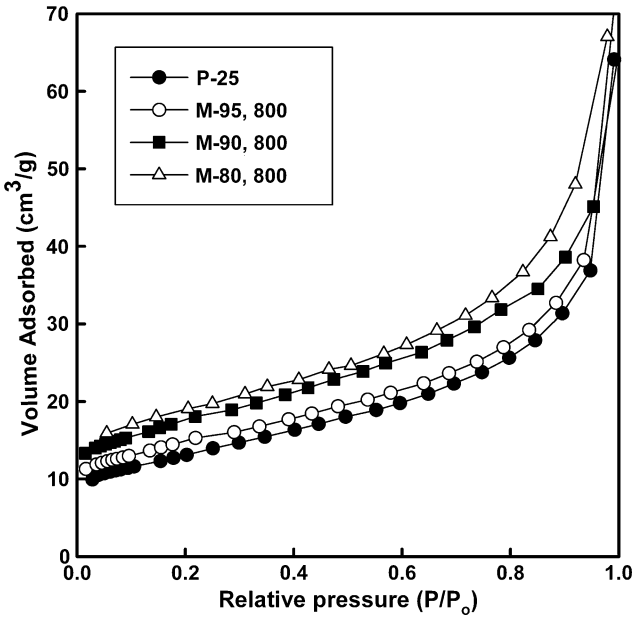

Fig. 2 Adsorption isotherms of nitrogen on P-25 and carbon-coated TiO_2 samples at 77 K

coated samples and P-25 are presented in Fig. 2. The pore sizes of the prepared samples and P-25 are listed in Table 2, which were calculated using the Barrett-Joyner-Halenda (BJH) method. The carbon-coated TiO_2 is mesoporous and has a pore size larger than that of P-25. In addition, the pore size distribution of carbon-coated TiO_2 was also broad. Table 3 shows the result of EDX analysis on the content elements of the carbon-coated samples. It was found that the carbon content of the prepared samples increases with an increasing PVA mixture ratio. FE-SEM images of P-25 and heat-treated P-25 (700, 800, and 900 °C) are shown in Fig. 3. We found that the original P-25 particles aggregated with the size of around 20–30 nm. Sintering of P-25 particle was observed at 700 °C along with the particle size increment larger than 100 nm and a large amount of small size particles. However, a negligible amount of small particles remained at above 800 °C. Figure 3 shows the rutile phase and particle size increasing with heat temperature. Figure 4a and b shows FE-SEM pictures of different TiO_2 and PVA ratios (80/20, 90/10) at various heat treatment temperatures ranging from 800 °C to 900 °C. Figure 4c illustrates the FE-SEM pictures for the sample with the

Table 3 The results of EDX analysis of carbon-coated TiO_2 samples

Sample code	Elmt	Element (%)	Sigma (%)	Atomic (%)
M-95, 800	C–K	4.52	0.48	14.78
	O–K	39.70	0.90	57.18
	Ti–K	55.78	0.83	28.04
M-90, 800	C–K	6.61	0.32	13.33
	O–K	48.41	0.55	64.79
	Ti–K	44.98	0.48	21.88
M-80, 800	C–K	10.66	0.30	19.05
	O–K	45.75	0.51	61.41
	Ti–K	43.59	0.45	19.54

TiO_2 and PVA ratio of 95/5 treated at 700 °C and 800 °C. The particles size range of 40 to 60 nm and a small amount of sintering were observed in the carbon-coated TiO_2 compared with the heat-treated P-25. The size of aggregated secondary particles determined by SEM was bigger than that of primary particles by XRD. As shown in Fig. 5, thin carbon layers are observed in the carbon-coated TiO_2 particles synthesized by the TiO_2 and PVA mixture ratio of 90/10 at heat treatment temperature of 800 °C. These images clearly showed that the carbon layer formed on TiO_2 has the proper thickness (2–3 nm) for the UV light to be reached onto the surface of photocatalyst.

Adsorption isotherm

The surface coverage for the organic compound with P-25 can be expressed as follows according to the Langmuir equation:

$$q = \frac{q_m bC}{(bC + 1)} \tag{2}$$

where b is the Langmuir constant related to the affinity of the binding sites, q is the amount of adsorbed material at equilibrium, q_m is the maximum adsorption capacity reflecting adsorption-desorption equilibrium, and C is the concentration of organic compound in solution. However, the adsorption isotherm of organic molecular on carbon-coated TiO_2 as adsorbent can be expressed according to the Freundlich equation as follows:

$$q = KC^{\frac{1}{n}} \tag{3}$$

Table 2 Structure parameters of P-25 and carbon-coated TiO_2 samples

Sample code	BET area (m^2/g)	Average pore size (nm)	Micropore volume (cm^3/g)	Mesopore volume (cm^3/g)
P-25	47.7	8.32	0.019	0.071
M-95, 800	51.4	13.74	0.022	0.078
M-90, 800	61.1	12.68	0.026	0.080
M-80, 800	65.7	10.98	0.028	0.088

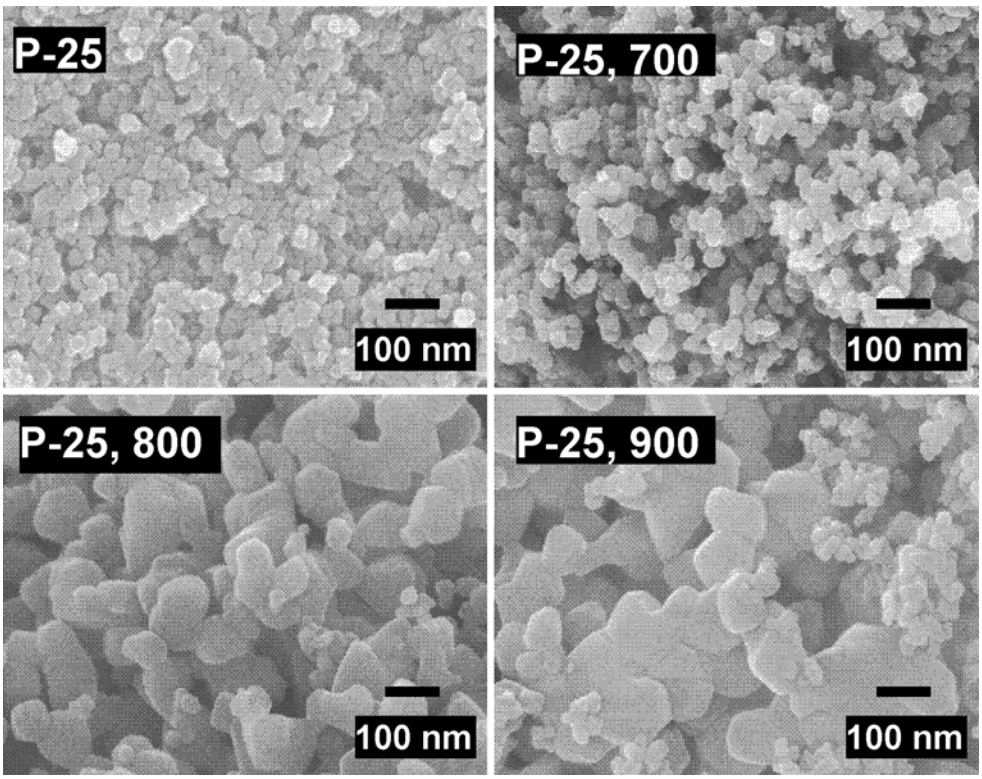

Fig. 3 FE-SEM images of the original and heat-treated P-25

where K is the Freundlich adsorption constant reflecting the adsorption capacity and n is the adsorption parameter. Figure 6 shows the adsorption equilibrium and kinetic for MB and BPA onto carbon-coated TiO_2 and P-25 at 25 °C.

As shown in Fig. 6a, the surface of carbon-coated samples is more heterogeneous than P-25. It is well known that the adsorption isotherm of organic compound on activated carbon fits the Freundlich equation well because the surface of activated carbon is commonly heterogeneous [15, 16]. To analyze the adsorption kinetics of MB and BPA, adsorption rate constant k was determined by using the pseudo second-order equation. This mathematical model satisfactorily approximated the adsorption kinetic data, since the corresponding correlation coefficients R^2 values were found to be higher than the pseudo first-order equation. As shown in Fig. 6b and Table 4, the adsorption rates of organic molecules onto carbon-coated samples are faster than that of P-25 under the same reaction condition.

Photocatalytic activity

The mechanism of the photocatalytic degradation using carbon-coated TiO_2 can be summarized as follows: (1) MB and BPA molecules are adsorbed on the carbon layer coated with TiO_2 and migrated to the surface of TiO_2; (2) the electron and hole pairs are formed on the surface of TiO_2 by UV light with light energy (hv) greater than its band gap energy (Eg); (3) the hole can give rise to hydroxyl radicals by reacting with H_2O or OH^-; and (4) the hydroxyl radicals, which are powerful oxidizing agents, can oxidize MB (or BPA) adsorbed onto the TiO_2 particles. The photocatalytic degradation process of MB (or BPA) at the surface of TiO_2 can be expressed as follows [17–20]:

$$\mathrm{MB_{sol}\ (or\ BPA_{sol})} + \mathrm{Carbon_{surface}} \xrightarrow{k_1} \mathrm{MB_{ads}\ (or\ BPA_{sol})} - \mathrm{Carbon_{surface}} \quad (4)$$

$$\mathrm{TiO_2} + h\nu \xrightarrow{k_2} \mathrm{h^+} + e^- \quad (5)$$

$$\mathrm{h^+} + \mathrm{H_2O_{ads}} \xrightarrow{k_3} \bullet\mathrm{OH} + \mathrm{H^+} \quad (6)$$

$$\mathrm{h^+} + \mathrm{OH^-} \xrightarrow{k_4} \bullet\mathrm{OH} \quad (7)$$

$$\mathrm{MB\ (or\ BPA)} + \bullet\mathrm{OH} \xrightarrow{k_5} \mathrm{CO_2} + \mathrm{H_2O} + \mathrm{inorganic\ \ ions} \quad (8)$$

Equation 8 shows the degradation of organic molecules that contain MB and BPA. Figure 7a shows the relative concentration decay curves of MB under UV irradiation for

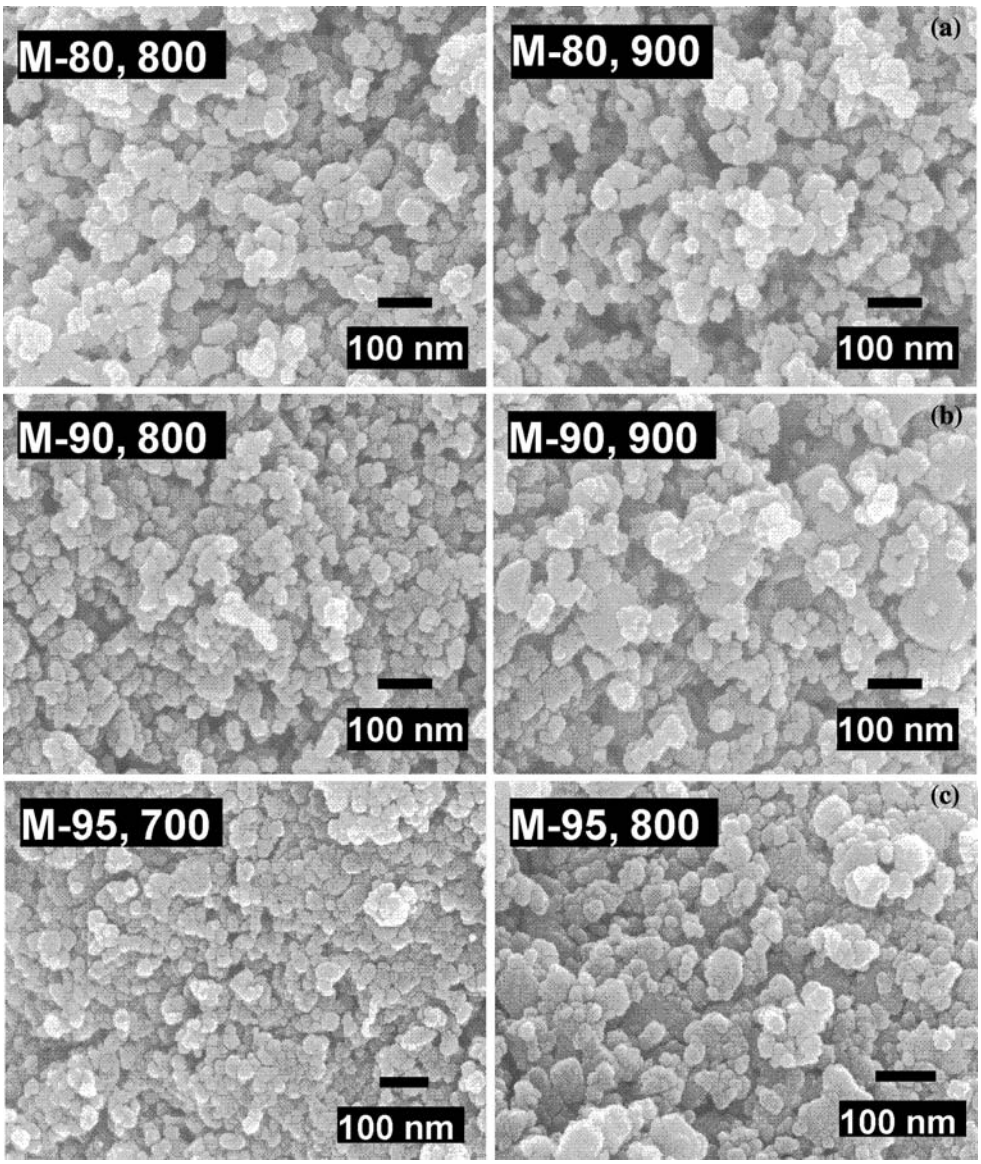

Fig. 4 FE-SEM images of different carbon-coated TiO_2 samples prepared at 800 and 900 °C: (**a**) TiO_2/PVA: 80/20 wt%; (**b**) TiO_2/PVA: 90/10; and (**c**) TiO_2/PVA: 95/5

the P-25 and carbon-coated TiO_2 catalysts at 25 °C. As shown in this figure, the concentration curves of MB decreased rapidly within 20 min and then gradually slowed down. This result may imply that the removal efficiency of MB was mainly dominated by the adsorptivity of catalysts at the initial stage and followed by the photodecomposition of catalysts. The photodecomposition of MB substantially followed the first-order reaction mechanism, and the reaction rate constants determined from the linear relationship between logarmetric relative concentration ($\log(C/C_0)$) and time (t) are listed in Table 5. In addition, the removal efficiency of dye molecule on carbon-coated catalysts was highly dependent on the mass ratios of carbon precursor and heat treatment temperature. The photodecomposition rate generally increased with mixing ratios at a constant heat treatment temperature. Increasing photodecomposition order was found to be M-80 > M-90 > M-95 at a heat treatment temperature of 800 °C. Also, the order of heat treatment temperatures was found to be 800 °C > 900 °C, 800 °C > 900 °C, and 700 °C > 800 °C for 80/20, 90/10, and 95/5 mixing ratios, respectively. Figure 7b shows the decay curves of BPA under reaction conditions similar to the previous case. Its photodecomposition order increased to M-90 > M-80 > M-95 at a heat treatment temperature of 800 °C, contrary to the photodecomposition order of MB. On the other hand, considering the photodecomposition of BPA with increasing heat treatment condition, the similar phenomena obtained in the above sections (MB) were observed for the same mixing ratios. In other words, the

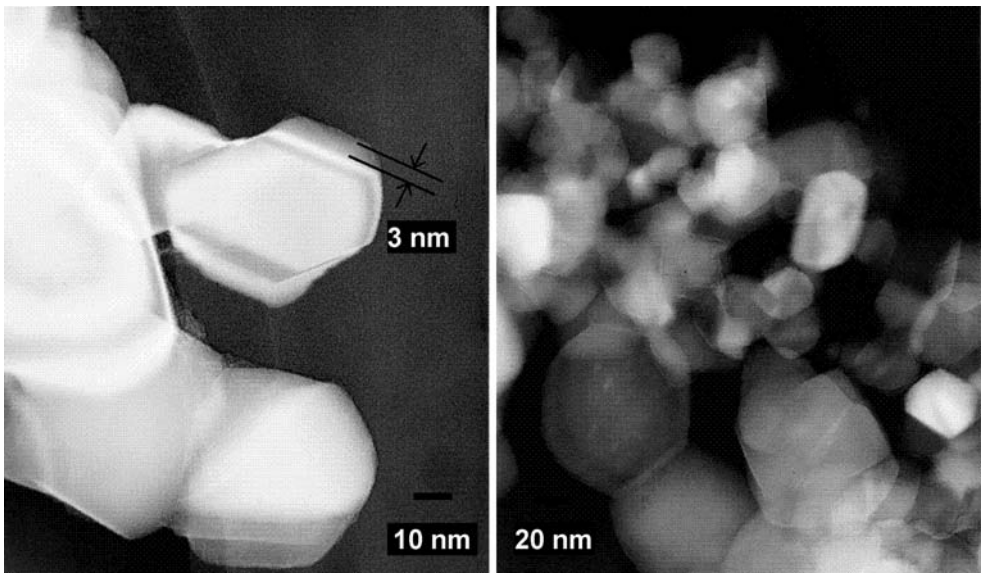

Fig. 5 TEM images of carbon-coated TiO_2 samples prepared at the mixture TiO_2/PVA ratio of 80/20 at 800 °C

samples prepared at lower treatment temperatures were more active than the catalysts synthesized at relatively higher temperatures. However, in the case of the same heat treatment temperature, M-90 (800 °C) shows a relatively higher photodecomposition efficiency compared to that of other mixing ratios. These results also revealed that although the photodecomposition rates of BPA were much lower than that of MB, the employed methods have a relatively high potential for the removal of the non-degradable molecules. Furthermore, the photocatalytic decomposition of BPA approached the first-order reaction. The reaction rate constants determined are also given in Table 5. It is known that the crystallinity of the anatase plays a key role in the photodecomposition of organic substances. Therefore, to determine the crystallinity of these samples, we studied FWHM of 101 X-ray diffraction line of anatase phase. Figure 8 shows the relation between decomposition rate constant k for MB and BPA with respect to FWHM of 101 diffraction line for carbon-coated anatase TiO_2. As shown in this figure, the sharp variation of the rate constant can be classified into two parts: (1) Part 1: drastically increased with a moderate increase of FWHM to approach the maximum rate constant and (2) Part 2: then rapidly decreased with an increasing FWHM. The maximum rate constants determined for MB and BPA were at around 0.35 ^{o} of FWHM. These results led us to conclude that the photocatalytic activity of the prepared sample is closely related to the crystallinity of the anatase phase. In other words, the improvement of crystallinity of anatase phase ascribed to the lower recombination reaction between electrons and holes was obtained as the heat treatment temperature increased in Part 1. This led to the relatively high photodecomposition of organic substances. On the other hand, in the case of Part 2, the main cause of the decrease of photocatalytic activity was the phase transition from anatase to rutile with increasing heat treatment temperature.

Conclusions

The carbon-coated anatase-type TiO_2 was successfully prepared for photodecomposition of organic compounds in aqueous solution. The removal efficiency of organic compounds on carbon-coated TiO_2 was considerably different depending on the mass ratios of carbon precursor and heat treatment temperature. We found that the mass ratio of 90/10 (TiO_2/PVA) and heat treatment of 800 °C are the suitable preparation conditions for the higher photodecomposition of non-degradable compounds. Compared to the original P-25 catalyst, the prepared samples have much higher adsorption capacity and photocatalytic activity. However, the photodecomposition of prepared samples was lower than P-25 because of lower dispersion of carbon-coated TiO_2 in water and less penetration of UV rays on the surface of carbon-coated TiO_2. The absorption of UV light by the coated carbon layer reduced the photocatalytic activity because the light reaching the surface of TiO_2 particles decreased. However, it is evident that the anatase structure of TiO_2 particles was stabilized at high calcination temperature, and it increased the adsorption amount of organic molecules by the coated carbon.

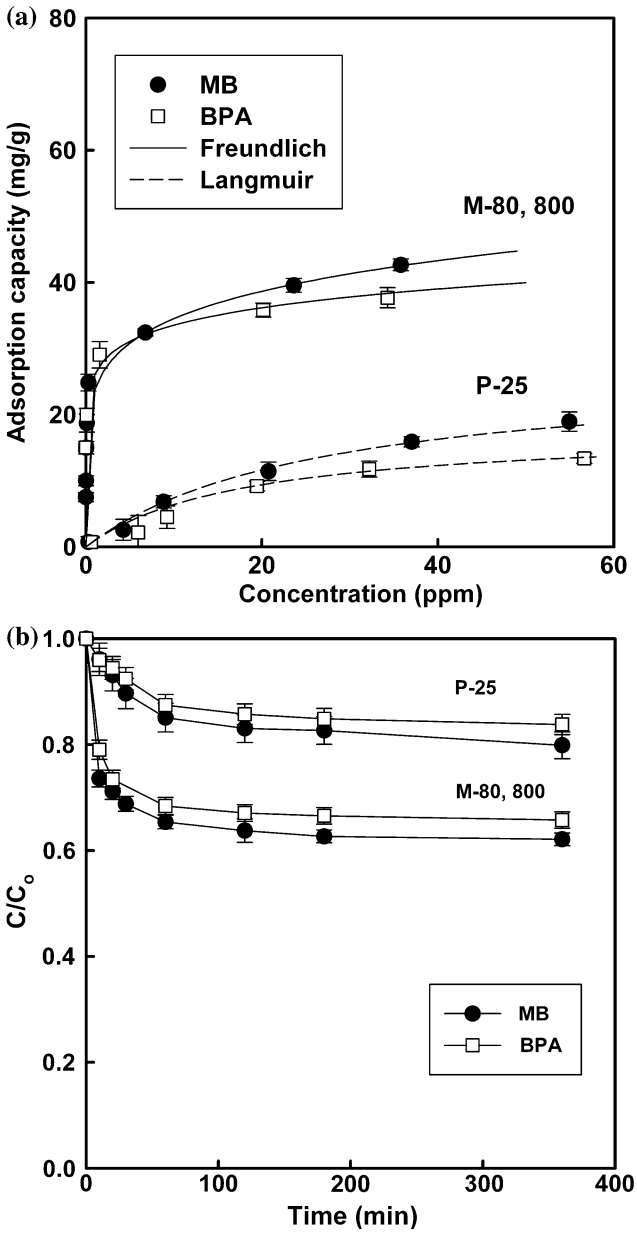

Fig. 6 Adsorption equilibrium (**a**) and kinetics (**b**) of MB and BPA on P-25 and carbon-coated TiO_2 at 25 °C

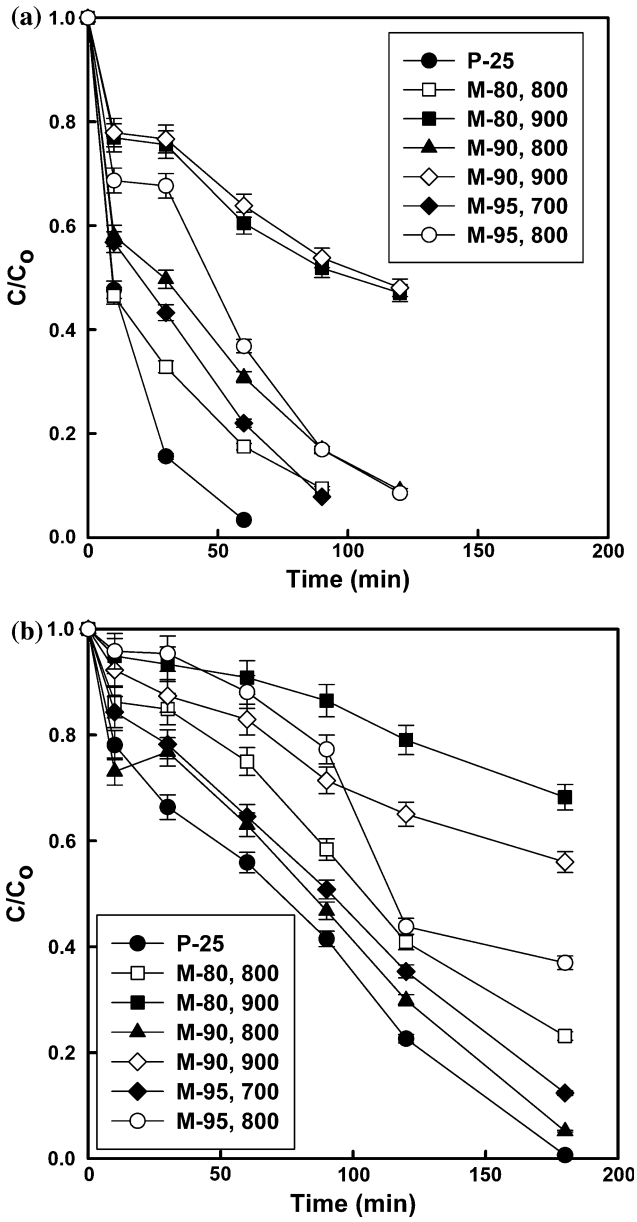

Fig. 7 Changes in the relative concentration (C/C_0) during the decomposition of MB and BPA caused by different photocatalysts under UV irradiation: (**a**) MB and (**b**) BPA

Table 4 Adsorption rate constants of MB and BPA on photocatalysts

Sample code	Material	k (g/(mg min))	R^2
P-25	MB	2.18×10^{-3}	0.996
P-25	BPA	3.06×10^{-3}	0.997
M-80, 800	MB	8.08×10^{-3}	0.999
M-80, 800	BPA	8.46×10^{-3}	1.000

Table 5 Rate constant k of photodecomposition of MB and BPA

Sample code	Rate constant k of MB (h^{-1})	Rate constant k of BPA (h^{-1})
P-25	3.381	1.216
M-80, 800	1.697	0.474
M-80, 900	0.150	0.128
M-90, 800	1.130	0.979
M-90, 900	0.168	0.194
M-95, 700	1.560	0.696
M-95, 800	0.989	0.305

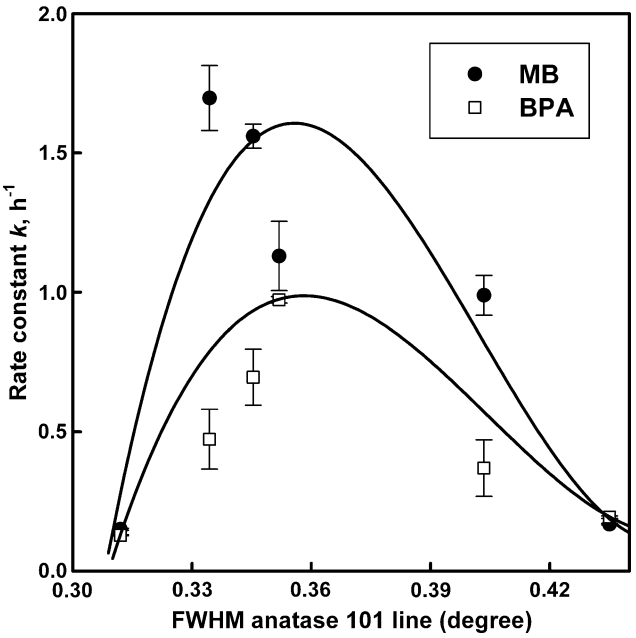

Fig. 8 Relation between the full width at half maximum intensity (FWHM) and the rate constant k for the photodecomposition of MB and BPA

References

1. Ohko Y, Ando I, Niwa C, Tatsuma T, Yamamura T, Nakamura T et al (2002) Environ Sci Technol 35:2365. doi:10.1021/es001757t
2. Lee JM, Kim MS, Kim BW (2004) Water Res 38:3605. doi:10.1016/j.watres.2004.05.015
3. Tryba B, Morawski AW, Tsumura T, Toyoda M, Inagaki M (2004) J Photoch Photobiol Chem (Kyoto) 167:127
4. Tsumura T, Kojutani N, Umemura H, Toyoda M, Inagaki M (2002) Appl Surf Sci 196:429. doi:10.1016/S0169-4332(02)00081-8
5. Li Y, Zhang S, Yu O, Yin W (2007) Appl Surf Sci 253:9254. doi:10.1016/j.apsusc.2007.05.057
6. Tsumura T, Kojitan N, Izumi I, Iwashita N, Toyoda M, Inagaki M (2002) J Mater Chem 12:1391. doi:10.1039/b201942f
7. Tsumura T, Kojitan N, Umemura H, Toyoda M, Inagaki M (2002) Appl Surf Sci 196:429. doi:10.1016/S0169-4332(02)00081-8
8. Torimoto T, Okawa Y, Takeda N, Yoneyama H (1997) J Photoch Photobiol Chem (Kyoto) 103:153
9. Inagaki M, Kojin F, Tryba B, Toyoda M (2005) Carbon 43:1652. doi:10.1016/j.carbon.2005.01.043
10. Zhang X, Zhou M, Lei L (2006) Carbon 44:325. doi:10.1016/j.carbon.2005.07.033
11. Inagaki M, Imai T, Yoshikawa T, Tryba B (2004) Appl Catal B Environ 51:247. doi:10.1016/j.apcatb.2004.02.017
12. Inagaki M, Hirose Y, Matsunaga T, Tsumura T, Toyoda M (2003) Carbon 41:2619. doi:10.1016/S0008-6223(03)00340-3
13. Li Y, Zhang S, Yu O, Yin W (2007) Appl Surf Sci 253:9254. doi:10.1016/j.apsusc.2007.05.057
14. Fiona L, Brian R, Heather M (2002) J Photoch Photobiol Chem (Kyoto) 148:137
15. Jaroniec M, Madey R, Choma J, Piotrowska J (1988) J Colloid Interface Sci 125(2):561. doi:10.1016/0021-9797(88)90022-7
16. Podko′scielny P, Nieszporek K, Szabelski P (2006) Colloid Surf A Physicochem Eng Aspects 277:52
17. Konstantinou IK, Albanis TA (2004) Appl Catal B Environ 49:1. doi:10.1016/j.apcatb.2003.11.010
18. Hoffman M, Martin S, Choi W, Bahnemann D (1995) Chem Rev 95:69. doi:10.1021/cr00033a004
19. Peral J, Domenech X, Ollis D (1997) J Chem Technol Biotechnol 70:117. doi:10.1002/(SICI)1097-4660(199710)70:2<117::AID-JCTB746>3.0.CO;2-F
20. Poulios I, Aetopoulou I (1999) J Chem Technol Biotechnol 74:357. doi:10.1002/(SICI)1097-4660(199904)74:4<349::AID-JCTB5>3.0.CO;2-7